ASM Sc. J., 13, 2020
https://doi.org/10.32802/asmscj.2020.sm26(4.5)

MHD Stagnation Point Nanofluid Flow Pasta Permeable Stretching Sheet with Brownian Motion and Thermophoresis Effects

Aziera Nadiha Hazri, Khadijah Abdul Hamid, Siti Khuzaimah Soid, Ahmad Sukri Abd Aziz and Zaileha Md Ali*

Faculty of Computer and Mathematical Sciences, Universiti Teknologi MARA, 40450 UiTM Shah Alam, Selangor, Malaysia

The study of boundary layer stagnation point flow and heat transfer towards a permeable stretching surface saturated in a nanofluid with slips boundary conditions, applied magnetic field and thermal radiation in porous medium have been analysed numerically. A mathematical model of partial differential equations corresponds to momentum, energy and nanoparticle concentration is reduced into nonlinear ordinary differential equations using similarity variables. These ordinary differential equations are solved numerically by MAPLE software using Runge-Kutta-Fehlberg along with shooting technique. The influences of velocity ratio, permeability, thermophoresis and Brownian motion parameters on velocity, temperature and concentration profiles are analysed and presented graphically. It is found that the velocity ratio enhances the velocity profile but reduces both temperature and concentration profiles. However, the opposite results are observed for the permeability parameter. Furthermore, the thermophoresis and Brownian motion parameters elevate both the temperature profiles, but the thermophoresis increases, and the Brownian motion decreases the concentration profiles respectively.

Keywords: Boundary layer flow, slip permeable stretching sheet, MHD stagnation flow, thermophoresis, Brownian motion

I. INTRODUCTION

The idea of boundary layer pioneered by Ludwig Prandtl (Anderson, 2005) has been widely applied especially in engineering processes. For example, materials manufactured by extrusion where MHD has been considered in order to improve the extrusion production efficiency (Shaw et al. 2016; Hsiao, 2017; Zaman et al. 2017; Soid et al. 2017).MHD flow was investigated and analysed by Mukhopadhyay,(2013) and Agbaje et al. (2018). Plasmas and electrolyte are examples of the dynamics of electricity conducting fluids (Mabood et al. 2015). Stagnation-point flow is the combination of static and dynamic pressure. In addition, stagnation happens at a point when the velocity is zero (Shaughnessy et al. 2005). Ibrahim and Shankar, (2013) have studied about the presence of stagnation point in MHD boundary layer nanofluid flow. The theory on nanofluid was introduced by Choi and Eastman, (1995) and had become a very active area of exploration. The authors also stated that nanofluid might exhibit superior properties (Soid et al. 2017; Soid and Ishak, 2017).

Thermal radiation and heat transfer play significant and important effects especially in controlling heat transfer in industry (Hamad and Ferdows, 2012). Recently, the boundary layer nanofluid flow induced by a permeable surface has received significant considerations of several researchers (Azmi et al. 2017; Bejan and Nield, 2013). Slips are applied in technological matters such as internal cavities and polishing of artificial heart valves (Ibrahim and

*Corresponding author's e-mail: zaileha@tmsk.uitm.edu.my

Shankar, 2013). The velocity, temperature and nanoparticles concentration are influenced by the coefficient of slip. Motivated by the above observations, this paper extends the work done by Ibrahim et al. (2013) on the influences of velocity ratio, permeability, thermophoresis and Brownian motion parameters.

II. MATHEMATICAL FORMULATION

Consider the steady two-dimensional convective nanofluid flow over a permeable horizontal sheet in porous media in the presence of radiation. The horizontal plate is along x-axis and the y-axis is normal to the plate. In the positive direction of y-axis, the inflexible magnetic field of strength B_0 is activated together with the thermal radiation effect while porous plate is along the horizontal axis. T_∞ is considered as ambient temperature and C_∞ as ambient concentration where the body surface of horizontal plate is kept at a fix temperature T_w and concentration C_w. The sheet is stretched with velocity $u_w = ax$, where a is a constant, V_w is the wall mass flux and $U = cx$ is the ambient velocity where c is a constant.

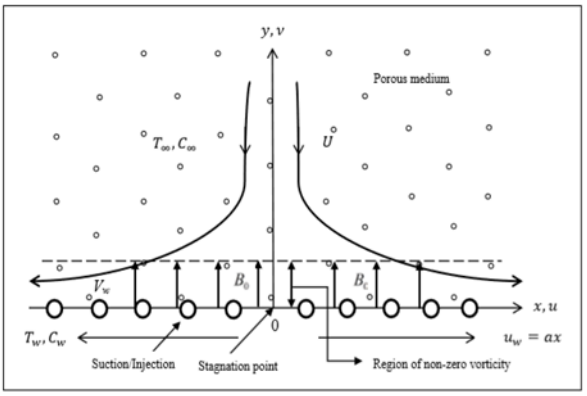

Figure 1. Schematic diagram of the problem

The boundary layer equations of continuity, momentum, energy and concentration are (Ibrahim *et al.*, 2013)

$$\frac{\partial u}{\partial x}+\frac{\partial v}{\partial y}=0 \tag{1}$$

$$u\frac{\partial u}{\partial x}+v\frac{\partial u}{\partial y}=U\frac{\partial U}{\partial x}+\upsilon\left(\frac{\partial^2 u}{\partial y^2}\right)+\frac{\sigma {B_0}^2}{\rho_f}(U-u) -\frac{\upsilon}{k}(u-U) \tag{2}$$

$$u\frac{\partial T}{\partial x}+v\frac{\partial T}{\partial y}=\alpha\left(\frac{\partial^2 T}{\partial y^2}\right)-\frac{1}{(\rho c)_f}\left(\frac{\partial q_r}{\partial y}\right)+ \frac{\mu}{\rho_f c_p}\left(\frac{\partial u}{\partial y}\right)^2+\left(\frac{\sigma {B_0}^2}{\rho_f c_p}\right)u^2+ \tau\left\{D_B\frac{\partial C}{\partial y}\frac{\partial T}{\partial y}+\frac{D_T}{T_\infty}\left(\frac{\partial T}{\partial y}\right)^2\right\} \tag{3}$$

$$u\frac{\partial C}{\partial x}+v\frac{\partial C}{\partial y}=D_B\frac{\partial^2 C}{\partial y^2}+\frac{D_T}{T_\infty}\frac{\partial^2 T}{\partial y^2} \tag{4}$$

where u and v are the velocity component along x-direction and y-direction respectively. $\upsilon=\mu/\rho_f$ is the kinematic viscosity where μ is dynamic viscosity of the fluid and ρ_f is the density of the base fluid, σ is the electrical conductivity, k is medium porosity, T is the temperature and $\alpha=\kappa/(\rho c)_f$ is the thermal diffusivity where κ is the thermal conductivity and $(\rho c)_f$ is heat capacity of the fluid. q_r is radiative heat flux, τ is stated as $(\rho c)_p/(\rho c)_f$, $(\rho c)_p$ is effective heat capacity of a nanoparticle and c_p is specific heat capacity at constant pressure. C, D_T, D_B are concentration, thermophoresis diffusion coefficient and Brownian diffusion coefficient respectively.

The corresponding boundary conditions are

$$y=0: u=u_w+L\frac{\partial u}{\partial y}, v=V_w, T=T_w+K_1\frac{\partial T}{\partial y}, C=C_w+K_2\frac{\partial C}{\partial y} \tag{5}$$

$$y\to\infty:\ u\to U=cx,\ T\to T_\infty,\ C\to C_\infty. \tag{6}$$

V_w is the wall mass flux where $V_w>0$ is injection and suction when $V_w<0$, both surface temperature, T_w and surface concentration C_w are constants. The condition with

no-slip is recovered when $L = K_1 = K_2 = 0$. L, K_1 and K_2 are the velocity, the thermal and the concentration slips factor. The mathematical formulation is simplified using similarity variables

$$\eta = \sqrt{\frac{a}{\upsilon}}\, y\,,\ \psi = \sqrt{a\upsilon}\, x\, f(\eta),\ \theta(\eta) = \frac{T - T_\infty}{T_w - T_\infty},\ \phi(\eta) = \frac{C - C_\infty}{C_w - C_\infty} \quad (7)$$

where r is similarity variable, ψ is stream function which defined as $u = \partial\psi / \partial y$ and $v = -\partial\psi / \partial x$. Both identically satisfy equation (1), $f(\eta)$is the dimensionless stream function, $\theta(\eta)$ is dimensionless temperature and $\phi(\eta)$is dimensionless concentration. The mathematical problem defined by equations (2)-(4) with boundary conditions (5)-(6) are transformed into ordinary differential equations as

$$f''' + f\, f'' - (f')^2 + \varepsilon^2 + M(\varepsilon - f') - \Omega(f' - \varepsilon) = 0 \quad (8)$$

$$\left(1 + \frac{4}{3}R\right)\theta'' + \Pr\, f\theta' + \Pr\, Nb\,\theta'\phi' + \Pr\, Nt\,(\theta')^2 = 0 \quad (9)$$

$$\phi'' + Le\, f\, \phi' + \frac{Nt}{Nb}\theta'' = 0 \quad (10)$$

where $\varepsilon = c/a$ is velocity ratio parameter, $M = \sigma B_0^{\,2} / \rho_f\, a$ is parameter of magnetic field, $\Omega = \upsilon / ak$ is permeability parameter, $R = 4\sigma^* T_\infty^{\,3} / k^* \kappa$ is a radiation parameter where σ^* is the Stefan-Boltzmann constant and k^* is the mean absorption coefficient, $\Pr = \upsilon / \alpha$ is a Prandtl number $Nb = (\rho c)_p D_B (C_w - C_\infty) / (\rho c)_f \upsilon$ is a Brownian motion parameter, $Nt = (\rho c)_p D_T (T_w - T_\infty) / (\rho c)_f \upsilon T_\infty$ is the thermophoresis parameter and $Le = \upsilon / D_B$ is a Lewis number.

The transformed boundary conditions are

$$\eta = 0:\quad f(0) = S,\quad f'(0) = 1 + Af''(0),\quad \theta(0) = 1 + B\theta'(0),\quad \phi(0) = 1 + C\phi'(0). \quad (11)$$

$$\eta \to \infty:\quad f'(\infty) \to \varepsilon,\quad \theta(\infty) \to 0,\quad \phi(0) \to 0 \quad (12)$$

where $S = V_w / -\sqrt{a\upsilon}$, $A = L\sqrt{a/\upsilon}$, $B = K_1\sqrt{a/\upsilon}$ and $C = K_2\sqrt{a/\upsilon}$ are suction parameter, velocity slip, thermal slip and concentration slip parameter respectively. The physical quantities in this problem are local skin friction coefficient C_f, local Nusselt number Nu_x and local Sherwood number Sh_x are declared as

$$C_f = \frac{\tau_w}{\rho u_w^{\,2}},\quad Nu_x = \frac{x q_w}{\kappa(T_w - T_\infty)},\quad Sh_x = \frac{x h_m}{D_B(C_w - C_\infty)} \quad (13)$$

where the wall shear stress τ_w the surface heat flux q_w and the surface mass flux h_m are given by

$$\tau_w = \mu\left(\frac{\partial u}{\partial y}\right)_{y=0},\quad q_w = -\kappa\left(\frac{\partial T}{\partial y}\right)_{y=0} + (q_r)_w,\quad h_w = -D_B\left(\frac{\partial C}{\partial y}\right)_{y=0}. \quad (14)$$

Solving the above equations, we obtained

$$C_f\sqrt{\mathrm{Re}_x} = f''(0),\ \frac{Nu_x}{\sqrt{\mathrm{Re}_x}} = -\left(1 + \frac{4}{3}R\right)\theta'(0),\ \frac{Sh_x}{\sqrt{\mathrm{Re}_x}} = -\phi'(0) \quad (15)$$

where $\mathrm{Re}_x = u_w x/\upsilon$ is the local Reynolds number.

III. RESULTS AND DISCUSSIONS

The nonlinear ordinary differential equations (8)-(10) with the boundary conditions (11)-(12) were solved numerically using “dsolve” MAPLE software. The procedure is based on Runge-Kutta-Fehlberg fourth and fifth order method with shooting technique.

A comparison with previously published papers Ibrahim and Shankar, (2013) and Hayat et al. (2011) are in a good agreement with the present results as shown in Table 1.

Table 1. Comparison of the skin friction coefficient $-f''(0)$ for various values of the velocity slip parameter

A	Hayat et al. (2011)	Ibrahim and Shankar, (2013)	Present results
0.0	1.000000	1.0000	1.0000
0.1	0.872082	0.8721	0.8721
0.2	0.776377	0.7764	0.7764
0.5	0.591195	0.5912	0.5912
2.0	0.283981	0.2840	0.2840
5.0	0.144841	0.1448	0.1448
10.0	0.081249	0.0812	0.0812
20.0	0.043782	0.0438	0.0438
50.0	0.018634	0.0186	0.0186

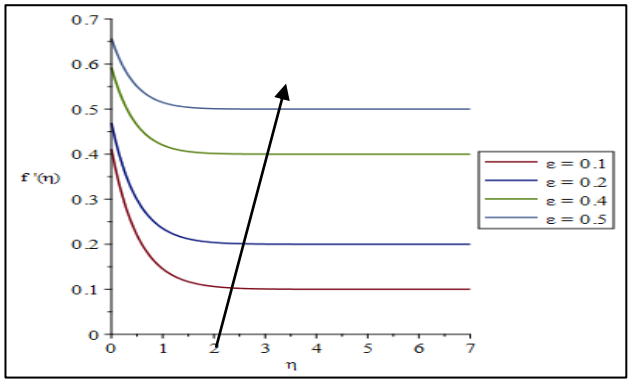

Figure 2. Velocity profiles $f'(\eta)$ for several values of ε with $M=1,\ \Omega=0.1, \Pr=6.2,$ $Le=5, R=Nt=Nb=0.5, S=A=B=1,\ C=1.$

Figure 2 exhibits as velocity ratio parameter increases, the velocity profile increases. This indicates that there is a slightly decline in the boundary layer with increase in ε which means the free stream velocity surpasses the stretching velocity.

Therefore, increment in the pressure and straining motion near the stagnation point leads to reduce the boundary layer thickness. The effect of velocity ratio parameter ε increment reveals that the temperature field decreased as depicts in Figure 3. As a result, the thermal boundary layer thickness decreases. Concentration boundary layer thickness is also reduced as the velocity ratio parameter ε increases as shown in Figure 4. This is due to the fall in the dimensionless temperature inside thermal boundary layer.

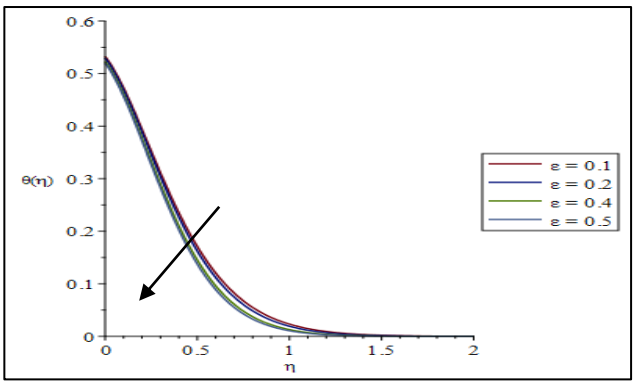

Figure 3. Temperature profiles $\theta(\eta)$ for several values of ε with $M=1, \Omega=0.1, \Pr=6.2,\ Le=5,$ $R=Nt=Nb=0.5, S=A=B=1,\ C=1.$

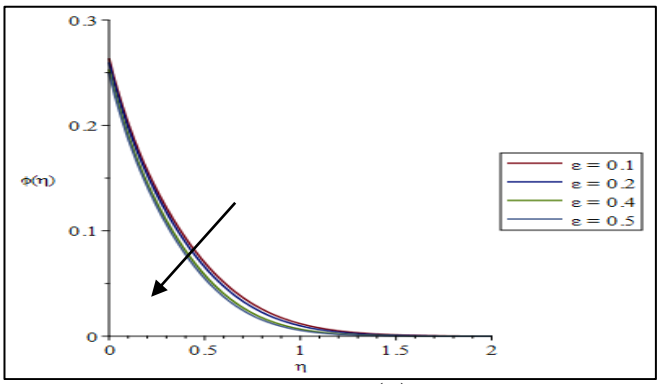

Figure 4. Concentration profiles $\phi(\eta)$ for several values of ε with $M=1,\ \Omega=0.1, \Pr=6.2,$ $Le=5, R=Nt=Nb=0.5, S=A=B=C=1.$

Figure 5 illustrates the decrement of velocity profile with different permeability parameter Ω due to a high Darcy force which slowing down the fluid in the boundary layer. However, both temperature and concentration profiles increase as the values of the permeability parameter Ω rises. At the same time, the gradient for both temperature and concentration distributions decrease with small changes as described in Figures 6 and 7. Hence, the changes in the permeability parameter Ω is insignificant to the boundary layer thickness of temperature and concentration profiles.

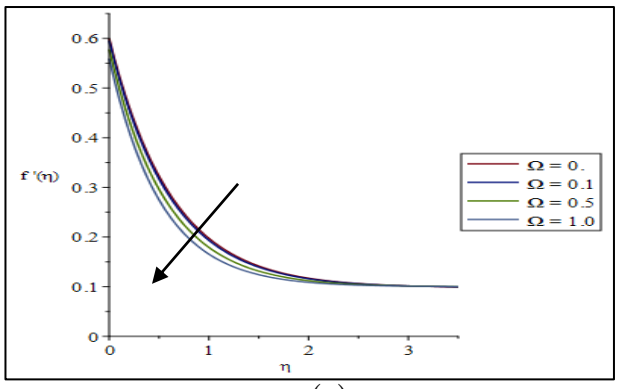

Figure 5. Velocity profiles $f'(\eta)$ for several values of Ω with $M = 1,\ \varepsilon = 0.1,\ \Pr = 6.2,$ $Le = 10,\ R = Nt = Nb = 0.5,\ S = A = 0.5.$

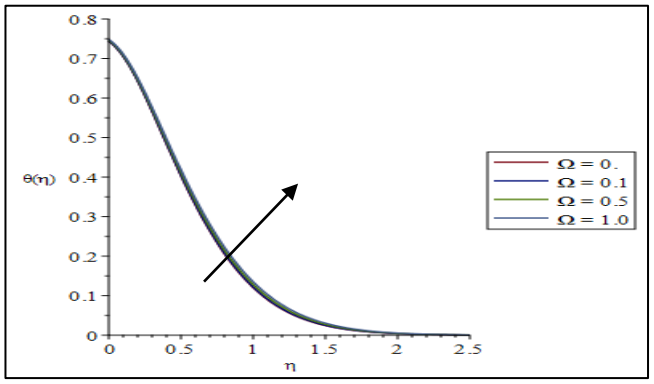

Figure 6. Temperature profiles $\theta(\eta)$ for several values of Ω with $M = 1, \varepsilon = 0.1, \Pr = 6.2,$ $Le = 10,\ R = Nt = Nb = 0.5,\ S = A = 0.5,\ B = 1.$

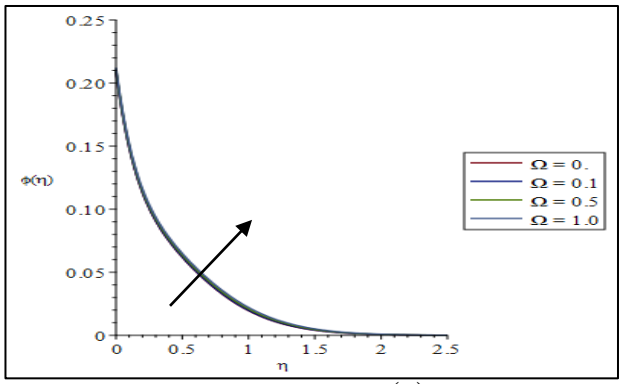

Figure 7. Concentration profiles $\phi(\eta)$ for several values of Ω with $M = 1, \varepsilon = 0.1, \Pr = 6.2,$ $Le = 10,\ R = Nt = Nb = 0.5,\ S = A = 0.5,\ B = C = 1.$

Figures 8 and 10 shows the same results as Brownian motion and thermophoresis parameters rise respectively. This is due to the collision between in the random of particles motion in a fluid encourages temperature enhancement. Figure 9 depicts the variation of concentration in response to a different value in Brownian motion parameter Nb. As the values of Nb increase, the concentration boundary layer thickness become thinner and close to the surface while oppositely for Figure 11 as the thermophoresis parameter Nt increases, the concentration field and boundary layer thickness also increases.

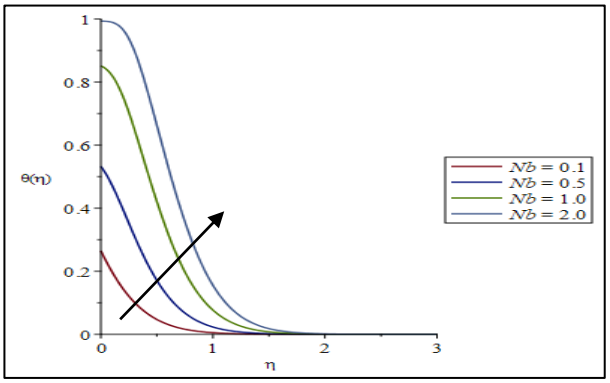

Figure 8. Temperature profiles $\theta(\eta)$ for several values of Nb with $M = 1, \varepsilon = 0.1, \Omega = 0.1,\ \Pr = 6.2,$ $Le = 5,\ R = Nt = 0.5,\ S = A = B = 1.$

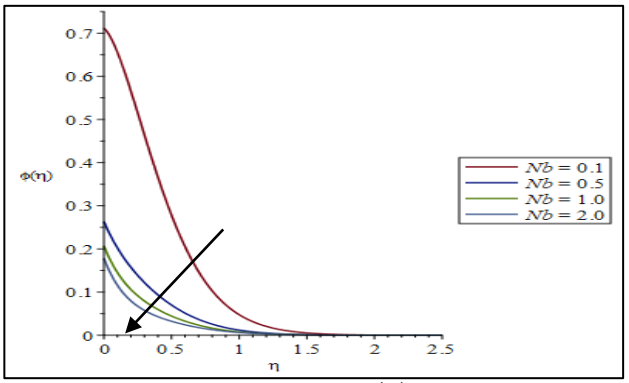

Figure 9. Concentration profiles $\phi(\eta)$ for several values of Nb with $M = 1, \varepsilon = 0.1, \Omega = 0.1,$ $\Pr = 6.2, Le = 5,\ R = Nt = 0.5,\ S = A = B = C = 1.$

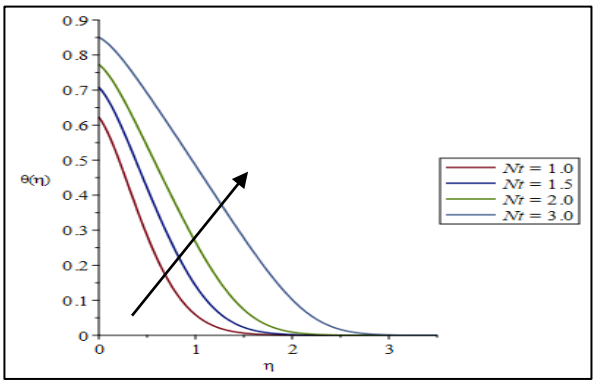

Figure 10. Temperature profiles $\theta(\eta)$ for several values of Nt with $M = 1, \varepsilon = 0.1, \Omega = 0.1,$ $\Pr = 6.2, Le = 5,\ R = Nb = 0.5,\ S = A = B = 1.$

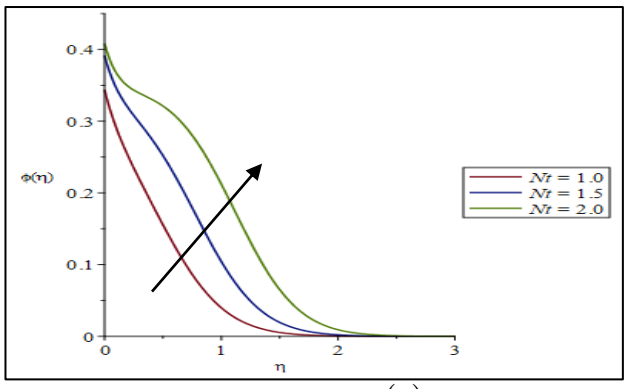

Figure 11. Concentration profiles $\phi(\eta)$ for several values of Nt with $M = 1, \varepsilon = 0.1, \Omega = 0.1, \Pr = 6.2,$ $Le = 5, R = Nb = 0.5, S = A = B = C = 1.$

IV. CONCLUSION

The effect of velocity ratio ε and permeability parameter Ω on the MHD boundary layer flow and heat transfer of a nanofluid over a permeable stretching sheet and slips effects with the presence of thermophoresis and Brownian motion were studied numerically.

In conclusion, the velocity ratio enhances the velocity profile but reduces both temperature and concentration profiles. However, the opposite results are observed for the permeability parameter. Furthermore, the thermophoresis and Brownian motion parameters elevate both the temperature profiles, but the thermophoresis increases, and the Brownian motion decreases the concentration profiles respectively.

V. ACKNOWLEDGEMENT

The authors acknowledge the financial support of Universiti Teknologi MARA under the Lestari Fund 600-IRMI/DANA 5/3/ LESTARI (0140/2016) and convey their sincere thanks to the reviewer for their comments and suggestions.

VI. REFERENCES

Agbaje, T. M., Mondal, S., Makukula, Z. G., Motsa, S. S. &Sibanda, P. (2018). A new numerical approach to MHD stagnation point flow and heat transfer towards a stretching sheet. Ain Shams Engineering Journal, 9(2), pp. 233-243.

Azmi, N.S.M, Soid, S.K., Abd Aziz, A. S. &Md Ali, Z. (2017). Unsteady mahnetohydrodynamics flow about a stagnation point on a stretching plate embedded in porous medium. Journal of Physics, 890, pp. 012013(1)-(6).

Anderson, J. D. (2005). Ludwig Prandtl's boundary layer. Physics Today,58(12), pp. 42-48.

Bejan, A. & Nield, D. A. (2013). *Convection in Porous Media*. New York: Springer.

Choi, S. U. S.& Eastman, J. A. (1995). Enhancing thermal conductivity of fluids with nanoparticles. ASME-Publications-Fed,231(66), pp. 99-106.

Hamad, M. A. A. & Ferdows, M. (2012). Similarity solution of boundary layer stagnation point flow towards a heated porous stretching sheet saturated with a nanofluid with heat absorption/generation and suction/blowing: A Lie group analysis. Communications in Nonlinear Science and Numerical Simulation, 17(1), pp. 132-140.

Hayat, T., Qasim, M. & Mesloub, S. (2011). MHD flow and heat transfer of a second grade fluid past a stretching sheet through a porous space. International Journal for Numerical Methods in Fluids, 66(8), pp. 963-975.

Hsiao, K. L. (2017). Combined electrical MHD heat transfer thermal extrusion system using Maxwell fluid with radiative and viscous dissipation effects. Applied Thermal Engineering, 112, pp. 1281-1288.

Ibrahim, W.& Shankar, B. (2013). MHD boundary layer flow and heat transfer of a nanofluid past a permeable stretching sheet with velocity, thermal and solutal slip boundary conditions. Computers & Fluids, 75, pp. 1-10.

Ibrahim, W., Shankar, B. & Nandeppanavar, M. M. (2013). MHD stagnation point flow and heat transfer due to nanofluid towards a stretching sheet. International Journal of Heat and Mass Transfer, 56(1), pp. 1-9.

Mabood, F., Khan, W. A. & Ismail, A. I. M. (2015). MHD stagnation point flow and heat transfer impinging on stretching sheet with chemical reaction and transpiration. Chemical Engineering Journal,273, pp. 430-437.

Mukhopadhyay, S. (2013). MHD boundary layer flow and heat transfer over an exponentially stretching sheet embedded in a thermally stratified medium. Ain Shams Engineering Journal,4(3), pp. 485-491.

Shaughnessy, E. J., Katz, I. M.& Schaffer, J. P. (2005). Introduction to Fluid Mechanics. New York: Oxford University Press New York.

Shaw, S. Kameswaran, P. K. &Sibanda, P. (2016). Effects of slip on nonlinear convection in nanofluid flow on stretching surfaces. Boundary Value Problems, 2016(2), pp. 1-11.

Soid, S.K., Ishak, A. & Pop. I. (2017). Unsteady MHD flow and heat transfer over a shrinking sheet with ohmic heating. Chinese Journal of Physics, 55, pp. 1626-1636.

Soid, S.K., Ishak, A. & Pop. I. (2017). Boundary layer flow past a continuously moving thin needle in a nanofluid. Applied Thermal Engineering, 114, pp. 58-64.

Soid, S.K. &Ishak, A. (2017). Axisymmetric flow of a nanofluid over a radially stretching/shrinking sheet

with a convective boundary condition. American Institute of physics, 1830, pp. 020006 (1)-(7).

Zaman, A. S., Abd Aziz, A. S. &Md Ali, Z. (2017). Double slip effects of Magnetohydrodynamic (MHD) boundary layer over an exponentially stetching sheet with radiation, heat source and chemical reaction. Journal of Physics, 890(1), pp. 012020(1)-(6).